



INSTITUTE OF
PAPER CHEMISTRY
Appleton Wisconsin

FLOW OF IDEAL FIBER SUSPENSIONS

Project 2570

Report Six

A Progress Report

to

MEMBERS OF GROUP PROJECT 2570

August 30, 1968

THE INSTITUTE OF PAPER CHEMISTRY
Appleton, Wisconsin

FLOW OF IDEAL FIBER SUSPENSIONS

Project 2570

Report Six

A Progress Report

to

MEMBERS OF GROUP PROJECT 2570

August 30, 1968

MEMBERS OF GROUP PROJECT 2570:

ALLIS-CHALMERS MANUFACTURING COMPANY

APPLETON WIRE WORKS CORP.

BELOIT CORPORATION

CONSOLIDATED PAPERS, INC.

CONTAINER CORPORATION OF AMERICA

EASTMAN KODAK COMPANY

FIBREBOARD CORPORATION

THE GLIDDEN COMPANY

INTERNATIONAL PAPER COMPANY

KIMBERLY-CLARK CORPORATION

KNOWLTON BROTHERS

LONGVIEW FIBRE COMPANY

THE MEAD CORPORATION

OXFORD PAPER COMPANY

RIEGEL PAPER CORPORATION

SCOTT PAPER COMPANY

UNION CAMP CORPORATION

WEST VIRGINIA PULP AND PAPER COMPANY

WEYERHAEUSER COMPANY

TABLE OF CONTENTS

	Page
SUMMARY	1
INTRODUCTION	2
EQUATIONS OF CONTINUITY AND MOTION	7
IDEAL STRESS-STRAIN RELATIONSHIPS	11
LAMINAR CHANNEL FLOW OF A HOOKEAN NETWORK IN WATER	16
TIME-SMOOTHED EQUATIONS OF TURBULENT SUSPENSION FLOW	26
MOMENTUM EXCHANGE IN A FIBER BALL-SIRUP SUSPENSION	33
DISCUSSION	40
ACKNOWLEDGMENT	43
NOMENCLATURE	44
LITERATURE CITED	47

FLOW OF IDEAL FIBER SUSPENSIONS

SUMMARY

Flow of fiber suspensions is dealt with on the basis of considering fibers and water as two phases of a mixture. It is assumed that both water and fibers can be treated as continua and that, in general, fibers and water move at different velocities. The resulting basic equations are similar to Emmons'. It is shown that the common compressibility equation used to describe the density-stress relationship for fiber mats reduces at very low stresses to Hooke's law. Applying the stress-strain relationship of the Theory of Elasticity to the fiber phase under the condition of laminar flow in a channel, it is shown that the fiber network contracts in both lateral and flow directions, thus giving rise to the forming of a fiber-free layer of water close to solid walls and to a velocity of the network plug less than that of the water. The network deformation is shown to be a natural consequence of the stress-strain behavior of fiber networks under these flow conditions. Time smoothing of all equations results in new equations describing mean turbulent flow of fiber suspensions. They differ from those for Newtonian fluids in the appearance of additional Reynolds stresses and of a drag term depending on the velocity difference between fiber agglomerates and water. These equations are shown to reduce to those for Newtonian fluids in the case of a uniform fiber distribution and if the velocity difference approaches zero. It is suggested that these conditions are compatible and that they might be met at higher flow rates, as substantiated by recent experimental work.

INTRODUCTION

Flow of fiber suspensions is one of the most important secondary processes in the manufacturing of paper: Through the mechanism of fluid flow the fibers are dispersed and transported and then distributed across the sheetlike headbox jet. As a rule in high-speed operations, the product to be made will be only as uniform as the distribution of fibers in the jet. The hydrodynamic problem of flow of fiber suspensions has therefore received considerable attention from numerous workers in industry and academic research.

In general, papermaking fibers appear large in size when compared with molecular dimensions. The mechanism of fiber dispersion in flowing suspensions must therefore be associated with forces of predominantly hydrodynamic rather than molecular origin. Among the former, shearing stresses (originating near solid walls), normal stresses (occurring in regions of rapid accelerations), and, in naturally unstable flows, the Reynolds stresses are seen to be responsible for the spotty separation of fibers and water--a phenomenon usually referred to as flocculation.

Past studies, in accordance with the principle of trying to understand simple cases first, and because of an immediate need for the design of stock systems, have been concerned primarily with fully developed tube flow (1-13). Probably the most extensive investigation has been that carried out by the M.I.T. Hydrodynamics Laboratory under a TAPPI contract (4-6). A great many friction factor-Reynolds number correlations over a range of Reynolds numbers between 10^3 and 3.10^5 and velocity profiles obtained by the use of a flat-faced impact tube are reported. Attempts to interpret these profiles in terms of the Prandtl-von Kármán distribution failed to yield conclusive results. Some of the work at M.I.T. dealt with solid

particles (14). As it turned out, solid particles in suspension behave quite differently from fibers at the same Reynolds number. Work of considerable interest in connection with flocculation has been carried out at McGill University [e.g., (15)]. Another study also directed at flocculation is that of Wollwage (16). It includes the only known attempt to measure the attractive force between two fibers in water. While an attractive force is reported, it is rather small and may have been beyond the limits of accuracy of the apparatus used.

More recent work is described in Mih and Parker's paper (12) including the development of their Annular Purge Impact Probe. It is believed that the velocity profiles obtained with this probe are more reliable than those from any other existing probe. They show that at low "turbulent" flow rates a central network plug seems to exist whose extension decreases with increasing flow rate. The turbulent portions of these profiles seem to follow a logarithmic distribution as do Newtonian fluids-- however, with a lower von Kármán constant, also apparently varying with fiber consistency and fiber type. On the basis of certain similarities in orientation between their friction factors and those for rough pipes (but disregarding their relative position) Mih and Parker conclude that turbulent flow of fiber suspensions is analogous to turbulent flow of Newtonian fluids in rough pipes. Such a concept implies that the friction factor, with increasing flow rates, asymptotically reaches a constant value which varies only with fiber consistency, fiber type, and tube diameter. Also implicit are similar conclusions with respect to the velocity distribution.

The only essential difference in the experimental set-up between the work of Mih and Parker and that of Seely (13) is that the latter used a pipe loop with vertical legs for the pressure-difference and velocity-distribution measurements. Generally, fiber suspensions are nonbuoyant dispersions, which may give rise to asymmetrical fiber and velocity distributions when the body force is not in a

direction parallel to the observed flow. Seely's pressure drop-flow rate correlations suggest the existence of three distinct turbulent regions, designated: plug turbulence, damped turbulence, and Newtonian turbulence. The last-named is so designated because velocity profiles and friction factor vs. Reynolds number correlations in this region become the same as that of water alone. In the region of damped turbulence, the friction factor is practically constant over a wide range of flow rates (Fig. 1). The velocity distribution was found to be essentially logarithmic with an apparent von Kármán constant lower than its Newtonian value and increasing with flow rate until a limiting value equal to the Newtonian was reached. The critical flow rate or Reynolds number at which this occurs increases with the fiber consistency and depends also on the fiber type and tube diameter. From the critical Reynolds number on, turbulent momentum exchange is unaffected by the presence of the fibers. Seely's empirical formulas may be used to predict tube-flow pressure drops for cases within the approximate range of his experiments.

The concepts underlying the various empirical treatments mentioned above have been borrowed from the engineering analysis of Newtonian tube flow and the von Kármán constant, κ , is fitted so as to account for the presence of the fibers. In the light of Prandtl's mixing-length theory, reasonable arguments may be advanced as to why it is meaningful to correlate the variation of κ with flow rate and slurry consistency. But, as a matter of principle, this kind of approach is doomed to exhaust itself quickly because Prandtl's and von Kármán's starting equations (i.e., one or the other form of the equation of motion) are single-phase equations. As such, they cannot possibly be expected to include the effect on velocity distributions, etc., of a second phase (the fibers in the present case).

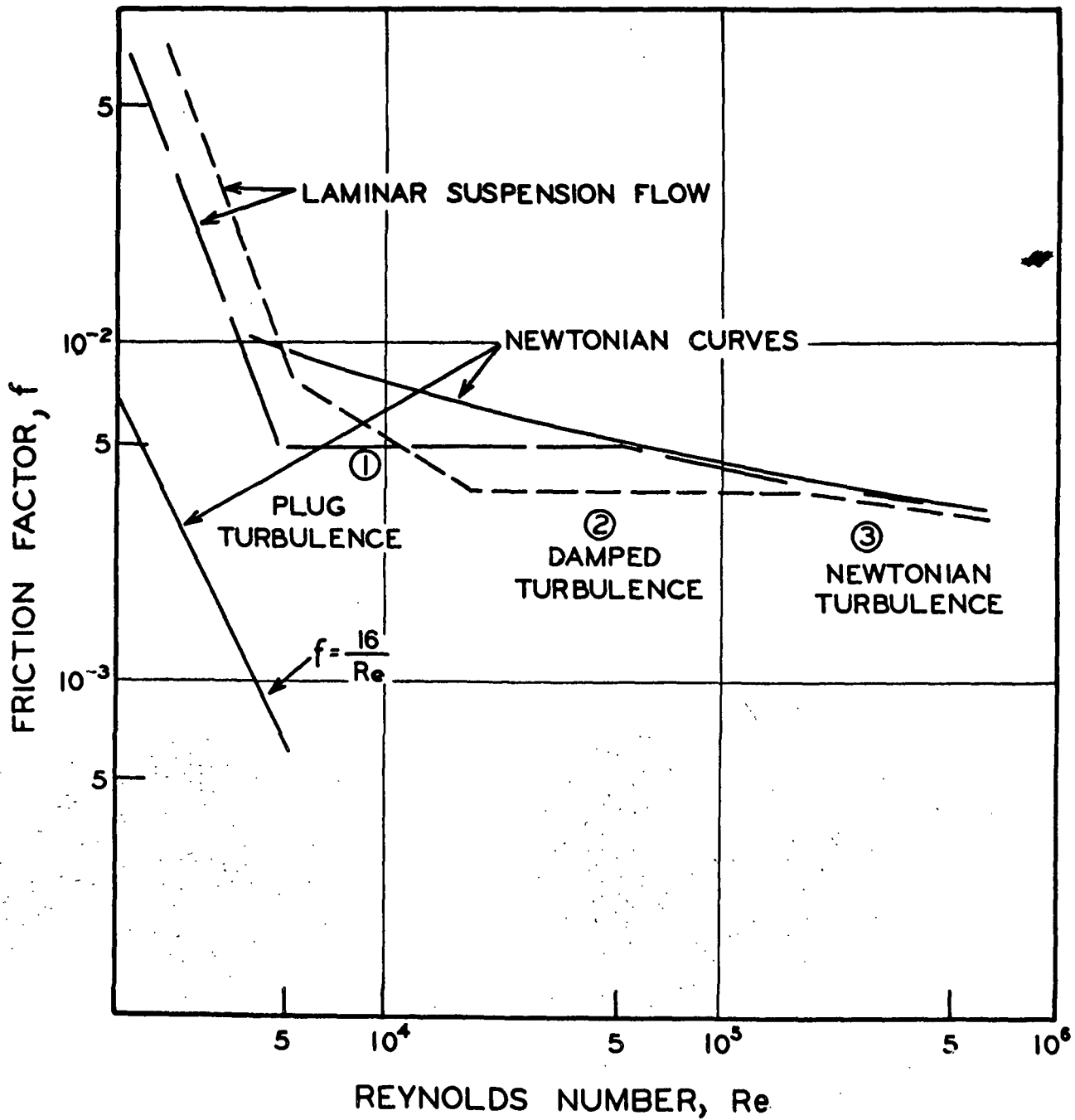


Figure 1. Characteristic Friction Factor-Reynolds Number Curves for Fiber Suspensions

Laminar plug flow has been treated and data provided by Daily and Bugliarello (3). Analytical attempts were made by Baines (10) and Meyer (11). The latter treatment is based on the rather arbitrary model of a brush and its observed deformation under shear, but nevertheless leads to predictions of the annulus thickness compatible with Daily's results. Also predicted are separate tube diameter and viscosity effects which go in the right direction.

In the following text a new attempt will be made to describe the flow of fiber suspensions based on first principles. There will be an opportunity to show that normal and shear stresses occur quite naturally in the fibrous phase accompanied by strains which determine whether or not this network will fracture. It will also become clear that further observations of momentum exchange through moving network fragments or flocs is necessary and why the (ill-fated) fiber ball model could be very useful here.

EQUATIONS OF CONTINUITY AND MOTION

The flow of fluids is governed by the laws of conservation of mass and momentum usually expressed in the form of the equations of continuity,

$$\frac{\partial \rho}{\partial t} + \frac{\partial \rho v_i}{\partial x_i} = 0 \quad (1),$$

and motion,

$$\frac{\partial}{\partial t} \rho v_i + \frac{\partial}{\partial x_j} \rho v_i v_j = - \frac{\partial p}{\partial x_i} - \frac{\partial \tau_{ij}}{\partial x_j} + F_i \quad (2)*.$$

As usual, ρ = fluid mass per unit volume of fluid; v_i = velocity component in the direction of the x_i coordinate of a Cartesian system with the axes $x_1 \equiv x$, $x_2 \equiv y$, and $x_3 \equiv z$; p = fluid pressure driving force; τ_{ij} = stresses resulting from and resisting the deformation of a fluid element, e.g., τ_{xx} = x -directed normal stress on the face of a volume element perpendicular to the x -axis; τ_{yx} = x -directed shear stress in a plane perpendicular to the y -axis; and F_i = body force per unit volume of the fluid in the direction of the i -axis.

Equations (1) and (2) are the result of mass and force (= momentum) balances for a stationary volume element of very minute cubical dimensions. In that case, all local changes of mass and momentum fluxes can be accurately expressed in terms of their first-order differentials. Such a procedure is legitimate whenever the fluid is a continuum.

* Cartesian tensor notation was adopted here because of the geometry in the problem chosen for later solution and because of its greater convenience in such case as compared with vector notation. Notice that the summation convention applies,

$$\text{e.g., } \frac{\partial \tau_{ij}}{\partial x_j} = \frac{\partial \tau_{i1}}{\partial x_1} + \frac{\partial \tau_{i2}}{\partial x_2} + \frac{\partial \tau_{i3}}{\partial x_3}.$$

In turning our attention now to a fiber suspension, we observe that, neither the water nor the fiber phase is continuous; also, that in order to have, in a volume element of our consideration, a great number of fibers in their entire length, the cubicle has to be very large by comparison. In such case, and if we do not look too closely, we may consider the water and the fiber phases as two quasi-continua. When we further assume that such volume element is still very small as compared to the width of a channel, say, and also that rapid accelerations are absent, then equations similar to (1) and (2) apply approximately to each phase.

The true densities, ρ_Λ and ρ_Φ , of the water and fibers, respectively, are related to those of their apparent densities in the mixture by

$$\rho_\Lambda \epsilon = \rho_\lambda \quad (3)$$

$$\rho_\Phi (1 - \epsilon) = \rho_\varphi \quad (4)$$

where ϵ and $(1 - \epsilon)$ are the respective fractions of the volume element occupied by water and fibers, respectively. Accordingly, the true density of the mixture is given by

$$\rho = \rho_\lambda + \rho_\varphi \quad (5)$$

Realizing that due to the finite macroscopic dimensions of the fibers (or the networks they might form) the velocities of the two phases will, in general, be different, the "continuity" equations for the two phases may be written as follows:

$$\frac{\partial \epsilon}{\partial t} + \frac{\partial \epsilon v_{\lambda i}}{\partial x_i} = 0 \quad (6)$$

$$-\frac{\partial \epsilon}{\partial t} + \frac{\partial (1 - \epsilon) v_{\varphi i}}{\partial x_i} = 0 \quad (7)$$

In incompressible flow, which was assumed, ρ_λ and ρ_ϕ are constant and therefore cancel out. The velocity components, $v_{\lambda i}$ and $v_{\phi i}$, of the water and fiber phases, respectively, are true average velocities within the volume element. Microscopic boundary effects are assumed to be taken care of in the averaging process.

Likewise, the equations of motion for the two phases must be set up for their apparent masses in the mixture under the effect of apparent forces acting on the elemental surfaces of the mixture. True and apparent pressures are related by

$$p_\lambda \epsilon = p_\lambda \quad (8)$$

$$p_\phi (1 - \epsilon) = p_\phi \quad (9),$$

where p_λ = normal force per unit face area of water and p_ϕ = normal force per unit face area of the fibers, while the total pressure, p , per unit face area of the mixture becomes

$$p = p_\lambda + p_\phi \quad (10).$$

Expressions analogous to those of (8) and (9) also hold for the stresses $\tau_{\lambda ij}$ and $\tau_{\phi ij}$, so that, for instance, for the water phase,

$$\tau_{\lambda ij} = \epsilon \tau_{\lambda ij} \quad (11)$$

with $\tau_{\lambda ij}$ as the Newtonian stress tensor in terms of velocity gradients and viscosity. When finally the body force is defined as the resultant force per unit volume of the mixture exerted by the water on the fibers, i.e., as

$$F_i = F_{\lambda i} \quad (12),$$

and gravity as a force is taken into account separately, we get the equations of motion in the form

$$\rho_{\Lambda} \left(\frac{\partial \epsilon v_{\lambda i}}{\partial t} + \frac{\partial}{\partial x_j} \epsilon v_{\lambda i} v_{\lambda j} \right) = - \frac{\partial p_{\Lambda}}{\partial x_i} - \frac{\partial \tau_{\lambda i j}}{\partial x_j} + \rho_{\Lambda} \epsilon g_i - F_{\lambda i} \quad (13)$$

$$\rho_{\Phi} \left(\frac{\partial (1-\epsilon) v_{\phi i}}{\partial t} + \frac{\partial (1-\epsilon) v_{\phi i} v_{\phi j}}{\partial x_j} \right) = - \frac{\partial p_{\Phi}}{\partial x_i} - \frac{\partial \tau_{\phi i j}}{\partial x_j} + \rho_{\Phi} (1-\epsilon) g_i + F_{\lambda i} \quad (14)$$

In accordance with the above definition, the forces available for the acceleration of the water phase are reduced by the amount $F_{\lambda i}$ used to contribute to the acceleration of the fiber phase. Under normal conditions, the water provides a buoyancy force, $-\rho_{\Lambda} (1-\epsilon) g_i$. When the fibers form network structures with the ability of withstanding small but finite relative flow without yielding, rise is given to a term $+\mu \epsilon (v_{\lambda i} - v_{\phi i})$ if the relative flow is in the range of the Darcy equation, which is assumed. The network is also capable of sensing the pressure gradient in flow direction of the fluid phase in the amount of $\frac{\partial}{\partial x_i} (1-\epsilon) p_{\Lambda}$. Therefore, we have

$$F_{\lambda i} = -\rho_{\Lambda} (1-\epsilon) g_i + \mu \epsilon (v_{\lambda i} - v_{\phi i}) + \frac{\partial}{\partial x_i} (1-\epsilon) p_{\Lambda} \quad (15)$$

Upon introducing Equation (15) and using the continuity equations [(6) and (7)] and Equation (5), Equations (13) and (14) assume the forms

$$\rho_{\Lambda} \epsilon \left(\frac{\partial v_{\lambda i}}{\partial t} + v_{\lambda j} \frac{\partial v_{\lambda i}}{\partial x_j} \right) = - \frac{\partial p_{\Lambda}}{\partial x_i} - \frac{\partial \tau_{\lambda i j}}{\partial x_j} + \rho_{\Lambda} g_i - \mu \epsilon (v_{\lambda i} - v_{\phi i}) \quad (16)$$

$$\rho_{\Phi} (1-\epsilon) \left(\frac{\partial v_{\phi i}}{\partial t} + v_{\phi j} \frac{\partial v_{\phi i}}{\partial x_j} \right) = - \frac{\partial (p-p_{\Lambda})}{\partial x_i} - \frac{\partial \tau_{\phi i j}}{\partial x_j} + (\rho - \rho_{\Lambda}) g_i + \mu \epsilon (v_{\lambda i} - v_{\phi i}) \quad (17)$$

To make the description of flow of fibrous suspensions complete, the boundary conditions must be stated; further, the stress tensor, $\tau_{\lambda_{ij}}$, in terms of velocity gradients of the fluid phase, the stress tensor, $\tau_{\varphi_{ij}}$, in terms of the network strains, and an equation describing the state of the fiber network must be known in addition to the above Equations (6), (7), (16), and (17). When the last two equations are added and use is made of Equations (3)-(5), the following equation results:

$$\rho \left(\frac{\partial v_{\varphi i}}{\partial t} + v_{\varphi j} \frac{\partial v_{\varphi i}}{\partial x_j} \right) + \rho \Lambda \epsilon \left[\frac{\partial}{\partial t} (v_{\lambda i} - v_{\varphi i}) + v_{\lambda j} \frac{\partial v_{\lambda i}}{\partial x_j} - v_{\varphi j} \frac{\partial v_{\varphi i}}{\partial x_j} \right] =$$

$$- \frac{\partial p}{\partial x_i} - \frac{\partial}{\partial x_j} (\tau_{\lambda_{ij}} + \tau_{\varphi_{ij}}) + \rho g_i \quad (17a)$$

Only in the case of identical fiber and fluid velocities, i.e., when $v_{\varphi i} = v_{\lambda i}$, the second group of convective terms vanishes and Equation (17a) reduces into Equation (2). It may very well be that in such case also $\tau_{\varphi_{ij}} \rightarrow 0$, which would mean that the role of the fibers as separate vehicles of momentum transfer is no longer distinguishable from that of the water.

In setting up these equations, profitable advantage has been derived from Emmons' (17) and Nelson's (18) papers.

IDEAL STRESS-STRAIN RELATIONSHIPS

Flow of fluids is accompanied by continuous deformations of all fluid elements involved. The stresses resisting deformation are proportional to the rate of deformation or velocity gradients. For Newtonian fluids, the proportionality factor is known as the viscosity. There are altogether nine component stresses: three normal stresses and six shear stresses, the latter of which reduce to three pairs, and there are nine rates of deformation. The number of components make fluid stress and rate of deformation each a tensor, which, for Newtonian fluids and certain non-Newtonian model rheological fluids, are known (19, 20). Seldom in practical applications are all components of equal significance.

The stresses resisting deformation in solids depend on the extent of deformation a solid body undergoes. Within the range of proportionality of stress and strain, the factors of proportionality are the modulus of elasticity, \underline{E} , for the normal stresses and the shear modulus, \underline{G} , for the shear stresses. \underline{G} is related to the elasticity modulus, \underline{E} , and the Poisson ratio, σ , by the equation

$$G = \frac{E}{2(1 + \sigma)} \quad (18)$$

Stresses and strains in solids are again tensors, whose components are particularly well known for solids under deformation in the range of Hooke's law (19, 21). In contrast to the fluids, which, in general, can be continuously deformed without any nonreversible effect on their molecular structure, solids fail when their breaking stresses are exceeded, thus causing structural changes which are nonreversible.

In light of these remarks, we are led to conclude that we are well prepared as regards the fluid stresses $\tau_{\lambda_{ij}}$ in Equation (16), but seemingly rather ill prepared regarding the stresses $\tau_{\phi_{ij}}$ in Equation (17) for the fibrous phase. Stress-strain data of fibrous systems in the range of stresses as might be expected under flow conditions are unfortunately not available, and even the understanding of their behavior under compressive stresses of a comparatively high level has not progressed very far. A comprehensive representation of the state of affairs in this matter is contained in Han's review (22).

We proceed to show that an established compressibility relationship frequently used in filtration work with papermaking fibers, when extrapolated to very low stresses, yields a relationship between stress and strain equivalent to Hooke's law. In a compressibility experiment, the mass m of the fiber mat remains constant so that

$$cV = c_0 V_0 = m \quad (19) ,$$

where c_0 and V_0 are the initial mat density and volume, respectively, and where c and V are these values after the application of a compressive normal stress. In such case, V becomes smaller than V_0 by ΔV , and upon introducing the volume dilatation, e , by Equation (20),

$$e = \Delta V / V_0 \quad (20) ;$$

Equation (19) can be expressed as

$$e = 1 - \frac{c_0}{c} \quad (21) .$$

A familiar correlation (22) connects mat density, c , and normal stress component, τ , in the form

$$c^{1/N} - c_0^{1/N} = M_b \tau \quad (22) ,$$

where \underline{M}_b and \underline{N} , the so-called compressibility constants, are found by fitting a curve through the data points. These constants vary distinctly with the pulp under investigation and the number of load-and-unload cycles; they also depend on whether or not the mat is constrained through lateral walls during compaction. Both \underline{M}_b and \underline{N} values are higher for laterally unconfined conditions (23), thus reflecting a higher mat density in such case.

Combining Equations (21) and (22), we obtain, upon assuming the stress τ to be very small,

$$e \approx \frac{NM_b}{c_0 \underline{1/N}} \tau + \text{higher order terms} \quad (23),$$

which holds provided $e \ll 1$. This expression is equivalent to Hooke's law, which states that stresses are proportional to strains. If we now make the far-reaching assumption that in the range of validity of Equation (23) fiber networks deform elastically (i.e., permanent creep, as observed at the much higher stress levels of repeated compressibility experiments, does not occur), we have gained an important advantage: The stress tensor, $\tau_{\phi_{ij}}$, of Equation (17) is identical to that of a Hookean solid body and is therefore known in terms of strains, from the Theory of Elasticity. Its Cartesian components are (21):

$$\left. \begin{aligned} \partial \xi / \partial x &= (1/E) [\tau_{xx} - \sigma(\tau_{yy} + \tau_{zz})] \\ \partial \eta / \partial y &= (1/E) [\tau_{yy} - \sigma(\tau_{zz} + \tau_{xx})] \\ \partial \zeta / \partial z &= (1/E) [\tau_{zz} - \sigma(\tau_{xx} + \tau_{yy})] \\ \partial \eta / \partial x + \partial \xi / \partial y &= (1/G) \tau_{xy} \\ \partial \zeta / \partial y + \partial \eta / \partial z &= (1/G) \tau_{yz} \\ \partial \xi / \partial z + \partial \zeta / \partial x &= (1/G) \tau_{zx} \end{aligned} \right\} (24),$$

where ξ , η , and ζ are the displacements in the x , y , and z directions, their partial derivatives representing strains (e.g., $\partial\xi/\partial x$, $\partial\eta/\partial y$) or angular displacements (e.g., $\partial\xi/\partial\eta$, $\partial\eta/\partial x$), and where the shear modulus, G , in terms of the elasticity modulus, E , and the Poisson ratio, σ , are given by Equation (18). It is understood that the fiber index, φ , to be attached to the τ 's of Equation (24) has been omitted for convenience.

The dilatation, e , can be expressed in terms of the strains by

$$e = \partial\xi/\partial x + \partial\eta/\partial y + \partial\zeta/\partial z \quad (25)$$

and through use of Equations (24) one obtains

$$E = \frac{c_0^{1/N} (1 - 2\sigma)}{NM_0} \quad (26)$$

as the modulus of elasticity of fiber networks obeying Equation (23). The stresses τ_{ij} of Equation (24) must satisfy the Beltrami-Mitchell compatibility equations, given in Sokolnikoff's book (21).

LAMINAR CHANNEL FLOW OF A HOOKEAN NETWORK IN WATER

Before entering into the analysis of channel flow, the reader may be reminded of certain phenomena which can be observed through Lucite tubes inside which fully-developed, laminar, steady flow of a fiber suspension, or, in short, plug flow, is taking place.

When the consistency is high enough (depending on the type and length of the wood pulp fiber used, e.g., $c_D \geq 0.0025$ g./ml.) and the original dispersion is good, the fibers move as a plug rather than as individuals. The plug boundary is separated from the tube wall by an annulus of apparently fiber-free water. When the motion stops, the annulus disappears, while the network expands elastically back to the full width of the tube. With regard to the friction factor, this regime of flow is characterized by showing considerably higher values than those of pure water (Fig. 1) and increasing with both consistency and tube diameter. Curves for the same fiber type but varying consistency and tube diameter appear to be parallel, their slope being steeper than that of the water line. Figure 2 represents an extract from Daily's (5) Long Lac fiber data. For lack of evidence to the contrary, we may assume that analogous observations would also hold for fully-developed laminar flow in a flat channel.

We proceed now with the analysis by means of the developed equations. Through the assumptions of fully-developed, two-dimensional, steady and laminar flow, all convective terms in the equations of motion for both the fluid and the fiber phases vanish by virtue of the continuity equations [(6) and (7)]. We assume a coordinate system as defined in Fig. 3, where flow is assumed to be in the direction of the longitudinal z -axis, while the channel's depth is measured in the x -direction. Equations (16) and (17) reduce into:

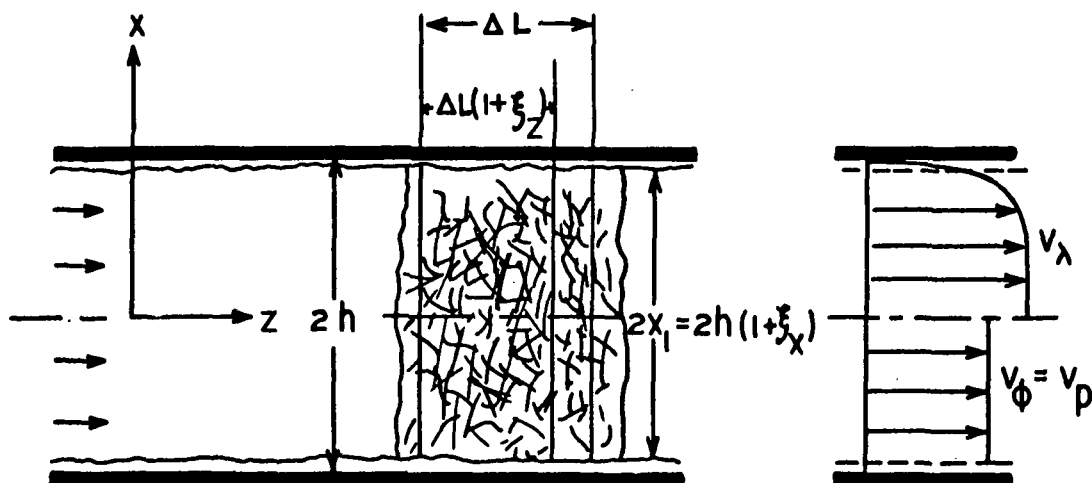


Figure 2. Coordinates and Plug Geometry for Flow in a Flat Channel

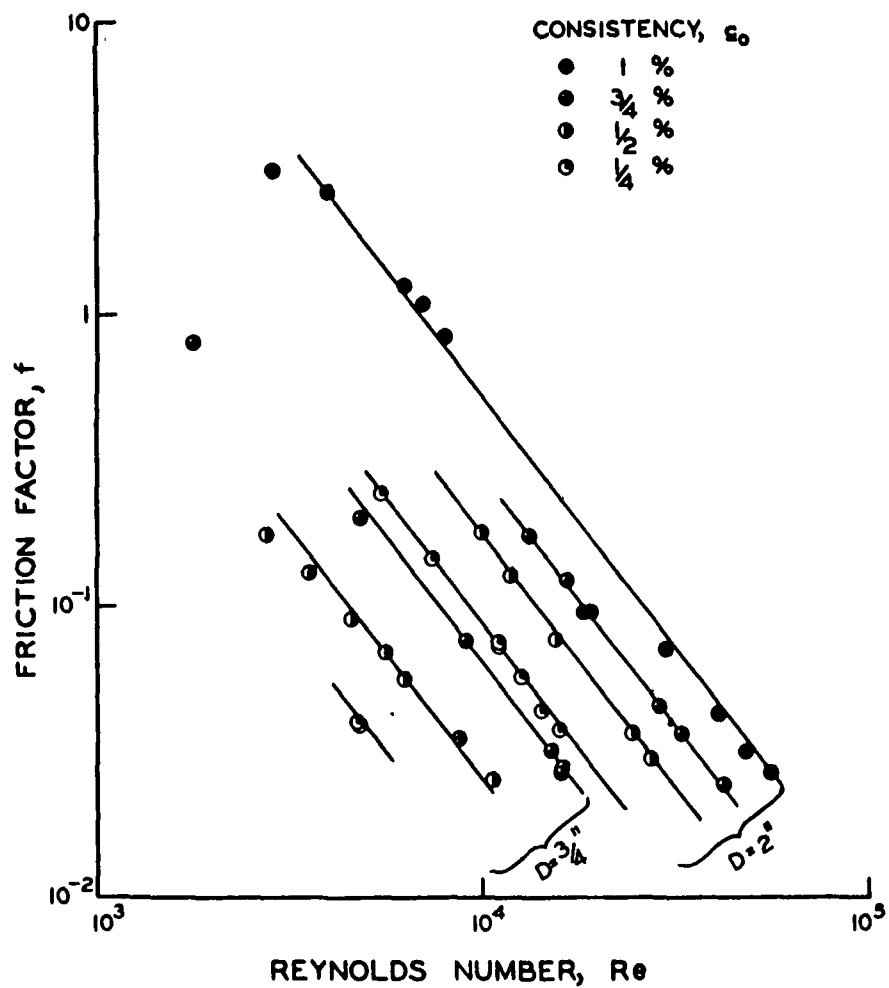


Figure 3. Friction Factor of Tube Flow of Long Lac Fibers in Water

$$-\frac{\partial p_{\Lambda}}{\partial x_i} - \frac{\partial \tau_{\lambda ij}}{\partial x_j} = D_i \quad (27)$$

$$\underline{i}, \underline{j} = 1, 2$$

$$-\frac{\partial (p-p_{\Lambda})}{\partial x_i} - \frac{\partial \tau_{\phi ij}}{\partial x_j} = -D_i \quad (28)$$

where the drag term was replaced by

$$D_i = \mu a \epsilon (v_{\lambda i} - v_{\phi i}) \quad (29)$$

and where also buoyancy was assumed. Equation (27) is the equilibrium condition for a volume element of the fluid phase, while Equation (28) is the same for a volume element of the fiber phase, i.e., of the fiber plug under the conditions of channel flow.

The drag term depends on the local relative velocity ($v_{\lambda i} - v_{\phi i}$) between water and fiber plug, and we are interested in how such a difference may arise. By combining the continuity equations [(6) and (7)] and executing the prescribed differentiations, the following expression is obtained:

$$\begin{aligned} \epsilon \left[\frac{\partial}{\partial x} (v_{\lambda x} - v_{\phi x}) + \frac{\partial}{\partial z} (v_{\lambda z} - v_{\phi z}) \right] + \frac{\partial \epsilon}{\partial x} (v_{\lambda x} - v_{\phi x}) + \frac{\partial \epsilon}{\partial z} (v_{\lambda z} - v_{\phi z}) \\ = - \left(\frac{\partial v_{\lambda x}}{\partial x} + \frac{\partial v_{\phi z}}{\partial z} \right) \quad (30) \end{aligned}$$

On the basis of our assumptions (which require $v_{\lambda x} = v_{\phi x} = 0$ and all derivatives with respect to \underline{z} to be zero), we conclude that continuity is satisfied even when $(v_{\lambda z} - v_{\phi z})$ and $\partial \epsilon / \partial x$ are finite. Further, that \underline{D}_i reduces to its component \underline{D}_z , i.e.,

$$D_1 = \begin{cases} D_x = \dots \\ D_z = \mu s_s (\bar{v}_{\lambda z} - v_{\phi z}) \end{cases} \quad (31)$$

where, for ϵ values close to unity, according to the combined Kozeny-Carman-Happel theory (24),

$$\mu s_s \approx \frac{2\mu S_v^2 (1 - \epsilon)}{\epsilon^3 [1 - \ln(1 - \epsilon)]} \quad (32)$$

with $\frac{S_v}{V}$ = mean surface area of fiber per unit volume of swollen fiber (specific surface area).

There are two possibilities for a relative motion between plug and water taking place. One is that the plug undergoes a continuous displacement, ζ , in z -direction such that

$$v_{\phi z} = v_{\lambda z} (1 + \zeta_z); \quad \zeta_z \equiv \partial \zeta / \partial z \quad (33)$$

A second possibility is that the plug moves with a constant true average velocity, v_p , which may depend on certain flow parameters, but should be independent of x . Thus,

$$v_{\phi z} - v_{\lambda z} = v_{\lambda z}(x) - v_p \quad (33a)$$

Since (33a) is in better agreement with observation, it will be adopted and the second part of Equation (31) assumes the form

$$\left. \begin{aligned} D_z &= D(x) = \mu a (v_{\lambda z} - \frac{\epsilon}{1 - \epsilon} v_p) \\ v_{\phi z} &= \epsilon v_{\lambda z}; \quad v_p = (1 - \epsilon) v_p \end{aligned} \right\} \quad (34)$$

where $V_{\lambda z}$ and V_p are superficial velocities, defined as the volume rate of flow of water and fibers, respectively, per unit area of the mixture. Notice that $V_{\lambda z}$ may vary with the distance x from the center plane of the channel, but should be a constant with respect to z . Depending upon whether $V_{\lambda z} > V_p$, the fibers drag the water or vice versa. For the time being, the plug velocity, $V_{\lambda z} = V_p$, is an unknown quantity.

Upon expressing $\tau_{\lambda ij}$ in terms of a Newtonian fluid and considering Equations (11) and (34), the two components of Equation (27), could be shown to reduce into the ordinary differential equation

$$-\frac{dp_{\Lambda}}{dz} + \mu \frac{d^2 v_{\lambda z}}{dx^2} - \mu a (v_{\lambda z} - \frac{\epsilon}{1-\epsilon} v_p) = 0$$

Between network plug and wall, i.e., in the fiber-free water layer. $\epsilon = 1$ and $a = 0$ by Equation (32). There the velocity distribution is described by

$$-\frac{dp_{\Lambda}}{dz} + \mu \frac{d^2 v_{\lambda z}}{dx^2} = 0$$

obtained by reducing Equation (35).

Suitable solutions (omitting subscripts where obvious and putting $dp_{\Lambda}/dz = p'_{\Lambda}$) are

$$v = \frac{1}{2\mu} (-p'_{\Lambda}) h^2 [1 - (\frac{x}{h})^2] - C_2 h (1 - \frac{x}{h}) ; \quad 0 \leq x \leq h$$

satisfying Equation (36) and the condition $v(h) = 0$. Assuming p'_{Λ} and C_2 to be constant, i.e., independent of x , Equation (35) is of the form of Brinkman's Equation (20) and has the solution

$$V = C_1 \cosh(\sqrt{ax}) - \frac{p'_\Lambda}{\mu a} + \frac{\epsilon}{1 - \epsilon} V_p ; \quad 0 \leq x \leq x_1$$

where

$$C_1 \cosh(\sqrt{ax_1}) = \frac{-p'_\Lambda}{2\mu} h^2 \left[1 - \left(\frac{x_1}{h} \right)^2 - \frac{2}{ah^2} \right] - C_2 h \left(1 - \frac{x_1}{h} \right) - \frac{\epsilon}{1 - \epsilon} V_p$$

$$C_2 \left[1 + \left(1 - \frac{x_1}{h} \right) \sqrt{ah} \tanh(\sqrt{ax_1}) \right] = \frac{-p'_\Lambda}{\mu} h \left[\frac{x_1}{h} + \frac{\sqrt{ah}}{2} \left(1 - \left(\frac{x_1}{h} \right)^2 - \frac{2}{ah^2} \right) \tanh(\sqrt{ax_1}) \right]$$

$$- \frac{\epsilon}{1 - \epsilon} \sqrt{a} V_p \tanh(\sqrt{ax_1})$$

The constants C_1 and C_2 were determined by use of the conditions that at the plug boundary where

$$x = x_1 = h(1 + \xi_x) ; \quad (\xi_x \equiv \partial \xi / \partial x) \quad (39)$$

both the velocity and the shearing stress are continuous.* The solution (38) further satisfies the symmetry condition, $dV/dx = 0$, in the middle of the channel at $x = 0$. The strain, $\partial \xi / \partial x$ of Equation (39) becomes negative for a fiber plug contracting in cross or x -direction.

The velocity distributions (37) and (38) yield important information regarding mean water and mean fiber velocity and wall shear stress.

We proceed to compute the mean water velocity, \bar{v}_λ , as defined by

$$\bar{v}_\lambda = \left(\int_0^{x_1} v dx + \int_{x_1}^h v dx \right) / h \quad (40)$$

* Note added while proofreading: Instead of continuity of shearing stress, a better condition would have been to satisfy continuity of pressure.

and obtain by use of Equations (37) through (39) and retaining only linear terms in ξ_x ,

$$\bar{v}_\lambda - \frac{\epsilon}{1-\epsilon} v_p (1+\xi_x) = \frac{c_1}{\sqrt{ah}} \sinh(\sqrt{a}x_1) + \frac{-p'_\lambda}{2\mu} h^2 \left(\frac{2}{3} + \frac{2(1+\xi_x)}{ah^2} \right) + c_2 h^2 \xi_x \quad (41)$$

with similar reductions in c_1 and c_2 as given by (38). Continuity of fiber flow requires that

$$v_p = \frac{1 - \epsilon_0}{\epsilon_0} \bar{v}_\lambda \quad (42)$$

where $\epsilon_0 = 1 - v_{c_0}$ and v_{c_0} = solid fraction of fibers in the mixing tank or stock chest used in the experimental set-up as the reservoir. By combining Equations (41) and (42) and taking into consideration the fact that the rate of suspension flow, Q (accessible through direct measurement) is given by

$$Q/2h = \bar{v}_\lambda + v_p = \bar{v}_\lambda / \epsilon_0 \quad (43),$$

an equation is obtained which, aside from the flow rate, Q , and pressure gradient $(-p'_\lambda)$, both known by direct measurement, contains two unknowns: the strain, $\xi_x = \partial \xi / \partial x$, and the void fraction, ϵ , in the fiber plug.

The shear stress at the channel wall, τ_h , may be obtained by differentiating Equation (37):

$$\tau_h = -\mu \left(\frac{dv}{dx} \right)_{x=h} = \frac{-p'_\lambda}{\mu} h - c_2 \quad (44),$$

which, upon expressing in c_2 the plug velocity, v_p , in terms of Equation (42) and making use of (43), again contains the unknown x -strain, ξ_x , and void

fraction, ϵ . By Equations (21) and (25), all strains must be known in order to relate void fraction and strain.

We now focus our attention on the network phase whose state of deformation is described by the stress-strain relationships (24) and the equilibrium conditions (28). The former reduce, in the two-dimensional case, to

$$\left. \begin{aligned} \frac{\partial \xi}{\partial x} &= (1/E)(\tau_{xx} - \sigma \tau_{zz}) \\ \frac{\partial \zeta}{\partial z} &= (1/E)(\tau_{zz} - \sigma \tau_{xx}) \\ \frac{\partial \xi}{\partial z} + \frac{\partial \zeta}{\partial x} &= (1/G)\tau_{zx} \end{aligned} \right\} \quad (45)$$

In terms of components, the equilibrium conditions become

$$\frac{\partial \tau_{zz}}{\partial z} + \frac{\partial \tau_{zx}}{\partial x} = D(x) \quad (46)$$

$$\frac{\partial \tau_{xx}}{\partial x} + \frac{\partial \tau_{zx}}{\partial z} = 0 \quad (47)$$

where the static pressure terms of Equation (28) have been included in the normal stress terms. It is understood that the index φ has been omitted for convenience.

The following conditions are compatible with observations and serve as conditions to the solutions of the above system of equations:

$$\left. \begin{aligned} \frac{\partial \tau_{zz}}{\partial z} &= \frac{\partial \tau_{zx}}{\partial z} = \frac{\partial \tau_{xx}}{\partial x} = 0 \\ \frac{\partial \xi}{\partial z} &= \frac{\partial^2 \zeta}{\partial z^2} = 0 \end{aligned} \right\} (48)$$

It is easy to verify that equations and conditions are satisfied by

$$\xi = Ax \quad (49a)$$

$$\zeta = \frac{1}{G} \int_0^x \int_0^x D dx dx + Bz \quad (49b)$$

$$\tau_{xx} = \frac{E}{1 - \sigma^2} (A + \sigma B) \quad (49c)$$

$$\tau_{zz} = \frac{E}{1 - \sigma^2} (\sigma A + B) \quad (49d)$$

$$\tau_{yz} = \int_0^x D dx \quad (49e)$$

where the constants A and B remain to be determined. There are no other forces present in the system except pressure forces and these, being nondirectional forces, are the same in both x and z directions. By use of (49c,d),

$$\tau_{xx} = \frac{E}{1 - \sigma^2} (A + \sigma B) = -(p - p_\Lambda) \quad (49c)$$

$$\tau_{zz} = \frac{E}{1 - \sigma^2} (\sigma A + B) = -(p - p_\Lambda) \quad (49d),$$

from which

$$A = B = -\frac{p - p_\Lambda}{E} (1 - \sigma) \quad (50),$$

and [by Equations (49a) and (49b)]

$$\frac{\partial \epsilon}{\partial z} = \frac{\partial \epsilon}{\partial z} \left(\frac{\partial \epsilon}{\partial z} \right)^{-1} \quad (51, 52)$$

follow. The strains in z and x directions are thus equal and negative, meaning that the network contracts in both the radial and the longitudinal directions. As a result, the void fraction, ϵ , will be lower than ϵ_0 in the reservoir. Considering signs, the relationship between void fraction, ϵ , and strains can be obtained by use of Equations (45), (51), and (52), as follows:

$$\epsilon = \epsilon_0 \left(1 - \frac{\sigma}{E} \right) \quad (53)$$

from which the void fraction in the channel

$$\epsilon = \epsilon_0 \left(1 - \frac{\sigma}{E} \right) \quad (53a)$$

is obtained. Upon entering (53a) into (42) and (-1) [whereby (42) is taken into account], a transcendental equation results, which can be solved for a series of data points [ϵ , $(-\frac{\sigma}{E})$] by numerical methods.

The last step concludes the radial portion of the analysis of channel flow. By (52) also, the $\frac{\partial \epsilon}{\partial z}$ is known, as well as the network pressure, $(p - p_A)$, and the stresses τ_{zz} and τ_{zx} , provided that the Poisson ratio, σ , and the modulus of elasticity, E , as defined by Equation (26) are known from independent experiments. The latter have to be conducted under unconfined conditions and interpreted in the same analysis, i.e., in the spirit of the system [Equations (45)-(48)].

TIME-SMOOTHED EQUATIONS OF TURBULENT SUSPENSION FLOW

It has been possible to deal with laminar suspension flow in a fairly rigorous fashion because of the simple final form into which the equations of motion and equilibrium reduced. As is known from the literature on Newtonian fluids, the description of turbulent flow in terms of continuity and momentum requires maintaining all terms even under the simplest geometric conditions. The solution of these equations is still considered an impractical if not impossible task. To an even greater extent, this is also true of Equations (6), (7), (16), and (17) supposedly describing flow of fiber suspensions, including the turbulent state of flow. Here, in addition to the water velocity, $\underline{v}_{\lambda i}$, and the pressure, \underline{p}_{λ} , also the fiber velocity, $\underline{v}_{\phi i}$, and the void fraction, ϵ , may vary with the space and time coordinates.

In past studies of fully-developed turbulent flow of Newtonian fluids in pipes and flat channels, the time-smoothed equations of motion and continuity provided the basis for celebrated engineering approaches to the problem of modeling the Reynolds stresses in terms of the time-smoothed velocities. Prandtl's mixing-length concept and von Kármán's similarity hypothesis [e.g., (19, 20)] lead to time-smoothed velocity and pressure distributions in close agreement with what can be measured by pitot tubes and pressure gages, respectively.

It is interesting to see what the time-smoothing process is doing to Equations (6), (7), (16), and (17). Then we'll reduce the resulting equations for the case of fully-developed flow in a flat channel and see which additional Reynolds stresses appear in this case. As usual, we put

$$\left. \begin{aligned}
 v_{\lambda i} &= \overline{v_{\lambda i}} + v'_{\lambda i} ; & p_{\lambda} &= \overline{p_{\lambda}} + p'_{\lambda} \\
 v_{\varphi i} &= \overline{v_{\varphi i}} + v'_{\varphi i} \\
 \epsilon &= \overline{\epsilon} + \epsilon' ; & \rho_{\varphi} &= \overline{\rho_{\varphi}} + \rho'_{\varphi}
 \end{aligned} \right\} \quad (54)$$

where the bar indicates a space-dependent time-mean value and the prime a space- and time-dependent fluctuation of the magnitude associated with the symbol. Thus, $v'_{\lambda i}$ is the time- and space-dependent fluctuation of the i th component of the water velocity, etc.

We begin with the continuity equations, (6) and (7), and obtain after time smoothing

$$\frac{\partial \overline{\epsilon}}{\partial t} + \frac{\partial}{\partial x_i} \left(\overline{\epsilon v_{\lambda i}} + \overline{\epsilon' v'_{\lambda i}} \right) = 0 \quad (55)$$

$$- \frac{\partial \overline{\epsilon}}{\partial t} + \frac{\partial}{\partial x_i} \left[\left(1 - \overline{\epsilon} \right) \overline{v_{\varphi i}} - \overline{\epsilon' v'_{\varphi i}} \right] = 0 \quad (56)$$

The same process transforms Equations (13) and (14) into

$$\begin{aligned}
 \rho_{\Lambda} \left\{ \frac{\partial}{\partial t} \left(\overline{\epsilon v_{\lambda i}} + \overline{\epsilon' v'_{\lambda i}} \right) + \frac{\partial}{\partial x_j} \left[\overline{\epsilon} \left(\overline{v_{\lambda i} v_{\lambda j}} + \overline{v'_{\lambda i} v'_{\lambda j}} \right) + \overline{v_{\lambda i} v'_{\lambda j} \epsilon'} + \overline{v_{\lambda j} v'_{\lambda i} \epsilon'} \right] \right\} \\
 = - \frac{\partial \overline{p_{\lambda}}}{\partial x_i} - \frac{\partial \overline{\tau_{\lambda i j}}}{\partial x_j} + \rho_{\Lambda} \overline{\epsilon} g_i - \overline{F_{\lambda i}} \quad (57)
 \end{aligned}$$

$$\begin{aligned}
 \rho_{\Phi} \left\{ \frac{\partial}{\partial t} \left[\left(1 - \overline{\epsilon} \right) \overline{v_{\varphi i}} - \overline{\epsilon' v'_{\varphi i}} \right] + \frac{\partial}{\partial x_j} \left[\left(1 - \overline{\epsilon} \right) \left(\overline{v_{\varphi i} v_{\varphi j}} + \overline{v'_{\varphi i} v'_{\varphi j}} \right) \right. \right. \\
 \left. \left. - \overline{v_{\varphi i} v'_{\varphi j} \epsilon'} - \overline{v_{\varphi j} v'_{\varphi i} \epsilon'} \right] \right\} = - \frac{\partial \overline{p_{\varphi}}}{\partial x_i} - \frac{\partial \overline{\tau_{\varphi i j}}}{\partial x_j} + \rho_{\Phi} (1 - \overline{\epsilon}) g_i + \overline{F_{\lambda i}} \quad (58)
 \end{aligned}$$

The underlined terms have evolved in the time-smoothing process, and we may refer to all of them as the Reynolds stresses of turbulent suspension flow. Before entering into a discussion of the meaning of some of these terms, we proceed to reduce the equations for the case of steady, fully-developed, incompressible flow in a flat channel, the coordinates being those of Fig. 2. Equations (55) and (56) become

$$\frac{\partial}{\partial x} \overline{\epsilon' v'_{\lambda x}} + \frac{\partial}{\partial z} \overline{\epsilon' v'_{\lambda z}} = 0 \quad (55a)$$

$$\frac{\partial}{\partial x} \overline{\epsilon' v'_{\varphi x}} + \frac{\partial}{\partial z} \overline{\epsilon' v'_{\varphi z}} = 0 \quad (56a)$$

where

$$\overline{v_{\lambda x}} = \overline{v_{\varphi x}} = \frac{\partial \overline{v_{\lambda z}}}{\partial z} = \frac{\partial \overline{v_{\varphi z}}}{\partial z} = \frac{\partial \overline{\epsilon}}{\partial z} = 0 \quad (59a)$$

has been taken into account.

In order to reduce the equations of motion, (58) and (59), into practical form, let us assume (1) that the suspension is in a state of buoyancy [so that the term $(\rho - \rho_{\Lambda}) \underline{g}_i$ vanishes]; (2) that the Reynolds stresses greatly exceed the yield stresses (tensile and shear) of the network fragments (flocs). The only possible stresses are those from the compacting pressure, $\overline{p} - \overline{p}_{\Lambda}$. Therefore, $\tau_{\varphi ij} = 0$; (3) that viscous wall friction is significant. Then, by making use of Equation (59) and the time-smoothed Equation (15), Equations (57) and (58) yield the following equations:

$$\rho_{\Lambda} \frac{\partial}{\partial x} \left[\overline{\epsilon v'_{\lambda z} v'_{\lambda x}} + \overline{v_{\lambda z} \epsilon' v'_{\lambda x}} \right] = - \frac{\partial \overline{p}_{\Lambda}}{\partial z} + \mu \frac{d^2 \overline{v_{\lambda}}}{dx^2} - \overline{D}_z \quad (60)$$

$$\rho_{\Lambda} \frac{\partial}{\partial x} \left[\overline{\epsilon v'_{\lambda z}} \right] = - \frac{\partial \overline{p}_{\Lambda}}{\partial x} - \overline{D}_x \quad (60a)$$

$$\rho_{\phi} \frac{\partial}{\partial x} \left[\left(1 - \bar{\epsilon}\right) \overline{v'_{\phi z} v'_{\phi x}} - \overline{v_{\phi z} \epsilon' v'_{\phi x}} \right] = - \frac{\partial(\bar{p} - \bar{p}_{\Lambda})}{\partial z} + \overline{D_z} \quad (61)$$

$$\rho_{\phi} \frac{\partial}{\partial x} \left[\left(1 - \bar{\epsilon}\right) \overline{v'^2_{\phi x}} \right] = - \frac{\partial(\bar{p} - \bar{p}_{\Lambda})}{\partial x} + \overline{D_x} \quad (61a)$$

By retaining the viscous drag term (as follows quite naturally) in its time-smoothed form, formal provisions are made for a time-mean net effect of viscous dampening on the mean turbulent motion.

Equations (60) through (61a) are significantly different from those for ordinary fluids mainly because of the drag terms, $\overline{D_i}$. However, they reduce into such equations if $\overline{\epsilon' v'_{\lambda x}} \rightarrow 0$ and if, by Equation (29), the time mean microscopic velocities $\overline{v_{\lambda i}}$ and $\overline{v_{\phi i}}$ of water and fiber, respectively, become closely the same. It is not unreasonable to speculate that their difference gradually disappears with increasing total energy of flow, i.e., with increasing Reynolds number, for example. Such an observation was made by Seely (13), and it would be a triumph of analysis if such an event and its dependence on certain gross parameters could be predicted. (The paper industry's interest in such a possibility lies in the fact that under those conditions an apparently ultimate state of hydrodynamic fiber dispersion is being reached.)

In view of Equation (55a) and by the mixing-length theory, we may write

$$\overline{\epsilon' v'_{\lambda x}} = \overline{l'_{\epsilon} l'_{\lambda}} \frac{1}{\bar{\epsilon}} \frac{d\bar{\epsilon}}{dx} \frac{d\overline{v_{\lambda}}}{dx} = \text{const.} \quad (62)$$

where l'_{ϵ} and l'_{λ} are the mixing lengths for the fiber density and water velocity distribution, respectively, and where in the vicinity of the wall

$$\overline{l'_{\epsilon} l'_{\lambda}} \approx (\kappa_1 s)^2 + \text{terms of higher order}; \quad s = h - x \quad (63)$$

by analogy with ordinary turbulent flow. We note that κ_1 will be different from von Kármán's κ . The only way the turbulent flux according to Equation (62) can disappear over the entire cross section is by virtue of $d\bar{\epsilon}/dx = 0$, that is, when the fibers are uniformly distributed. As may be seen, the two conclusions regarding fiber distribution and the equality of water and fiber velocities at high flow rates are quite compatible and also agreeable with the observed behavior of that of a quasi Newtonian fluid (13). In similar fashion, we put

$$\left. \begin{aligned} \bar{\epsilon} \overline{v'_{\lambda z} v'_{\lambda x}} &= l_{\lambda}^2 \frac{1}{\bar{\epsilon}} \left| \frac{d\bar{v}_{\lambda}}{dx} \right| \frac{d\bar{v}_{\lambda}}{dx} \\ (1 - \bar{\epsilon}) \overline{v'_{\varphi z} v'_{\varphi x}} &= l_{\varphi}^2 \frac{1}{1 - \bar{\epsilon}} \left| \frac{d\bar{v}_{\varphi}}{dx} \right| \frac{d\bar{v}_{\varphi}}{dx} \end{aligned} \right\} (64a, b)$$

where in terms of distance s from the channel wall,

$$\left. \begin{aligned} l_{\lambda} &\approx \kappa_2 s + \dots \\ l_{\varphi} &\approx \kappa_3 s + \dots \end{aligned} \right\} (65a, b)$$

with κ_2 close to von Kármán's κ , possibly.

It is somewhat more of a problem to find a suitable model for the time mean drag, $\overline{D_i}$. Upon introducing velocities and void fraction according to Equations (54) into Equation (29) and time smoothing, we obtain

$$\begin{aligned} \overline{D_i} &= \overline{\mu a \epsilon (v_{\lambda i} - v_{\varphi i})} \\ &= \mu \left[\bar{a} \left(\overline{v_{\lambda i}} - \frac{\bar{\epsilon}}{1 - \bar{\epsilon}} \overline{v_{\varphi i}} \right) + \bar{a} \left(\overline{\epsilon' v'_{\lambda i}} - \overline{\epsilon' v'_{\varphi i}} \right) \right] \end{aligned}$$

where the first and second terms are due to time - mean velocities and turbulent mass fluxes, respectively. The two drag components are

$$\overline{D}_x = \mu \overline{a} \left(\overline{v_{\lambda z}} - \frac{\overline{\epsilon}}{1 - \overline{\epsilon}} \overline{v_{\phi z}} + \overline{\epsilon' v'_{\lambda z}} - \overline{\epsilon' v'_{\phi z}} \right) \quad (66a)$$

$$\overline{D}_i = \mu \overline{a} (\overline{\epsilon' v'_{\lambda x}} - \overline{\epsilon' v'_{\phi x}}) \quad (66b)$$

where \overline{a} represents the viscous resistance of a network fragment or floc located at a distance \underline{x} from the center. In general, the resistance depends on the shape and, especially, on the number of bodies present in a unit of volume. It is easy to imagine that in turbulent motion the stablest mean shape for flocs of any size would be that of spheres. Assuming that simple Stokes drag is the basic mechanism involved, we can make profitable use of Seely's analysis of slow flow through porous spheres (25). It could be shown that for a "flocculation void fraction," $\overline{\epsilon}_f$, according to

$$\overline{\epsilon}_f = \frac{\overline{\epsilon} - \overline{\epsilon}_r}{1 - \overline{\epsilon}_r} \quad (67)$$

where $\overline{\epsilon}$ = local mean void fraction and $\overline{\epsilon}_r$ = mean void fraction in a floc of radius \underline{r} , the mean resistance, \overline{a} , becomes

$$\overline{a} = 9 \frac{(1 - \overline{\epsilon})}{1 - \overline{\epsilon}_r} \frac{a}{2ar^2 + 3} \quad (68)$$

with \underline{a} as defined by Equation (32), but with $\epsilon = \overline{\epsilon}_r$. The error committed in putting, for convenience, $\overline{\epsilon}_r \approx \overline{\epsilon}$ may not be too critical. In general, the mean flow resistance, \overline{a} , will vary with the \underline{x} -coordinate.

No attempt has been made up to this date of writing to carry the analysis any further. Incomplete and inexplicit as this concept may seem, it is nevertheless worthwhile to notice that the approach is both apparently original and consistent, and for that reason worthy of concentrated attention.

While mixing-length distributions are known for channel and tube flow of Newtonian fluids (19) which could be helpful in connection with Equations (60) and (64a), one can, for lack of data, only guess at the respective distributions for the fiber fluxes. Direct measurements of fiber or floc velocities in suspensions would require elaborate preparations and the study of events under fairly high speeds. Photographic methods would encounter difficulties with object identification and proper lighting. For these reasons and in order to obtain at least some related information, a suspension of fiber balls was placed in the Mason-Couette apparatus for observation of ball velocity distributions. The method of evaluation and some results of this study are described in the next chapter.

MOMENTUM EXCHANGE IN A FIBER BALL-SIRUP SUSPENSION

The same Fiber Flexibility Tester used for the previous work (26) was used for the observation of velocity distribution and momentum transfer between the fiber balls. While providing a large free area for easy observation, this instrument is not equipped for measuring the torque. Six hundred fiber balls of approximately 0.5-cm. diameter were suspended in the Couette apparatus with Karo sirup as flow medium. These fiber balls were picked out by hand from two batches of balls produced under exactly the same operating conditions in the Jacqueline apparatus. The fiber balls were then air dried before they were soaked in the Karo sirup. The purpose of doing this was to strengthen the structure of the balls and prevent them from losing fibers in the shear field. In the soaked condition of the ball-sirup mixture, there were about 0.66 balls/cm.³ of the mixture. To record the motion, a movie camera was mounted directly above the annulus. It was found by trial that, at inner and outer cylinder speeds of -26.2 and +23.3 cm./sec., respectively, a camera setting of 64 frames per second was suitable for the analysis of the velocities of the individual balls.

The movements of the fiber balls were traced with the help of a microfilm reader. With the speed of the movie camera known, the velocities of the fiber balls were calculated. The arbitrary references chosen were the inner cylinder and the right edge of each frame. By an arbitrary choice, whenever a fiber ball moved away from the inner cylinder, the radial velocity was designated as positive, and when it moved from right to left, the tangential velocity was also designated positive. For coordinates, see Fig. 4.

Assuming, as in Fig. 4, that an individual fiber ball travels from $P(x_1, y_1)$ to $P(x_2, y_2)$ and covers a distance \underline{s} , the velocity vector of motion between points P_1 and P_2 is:

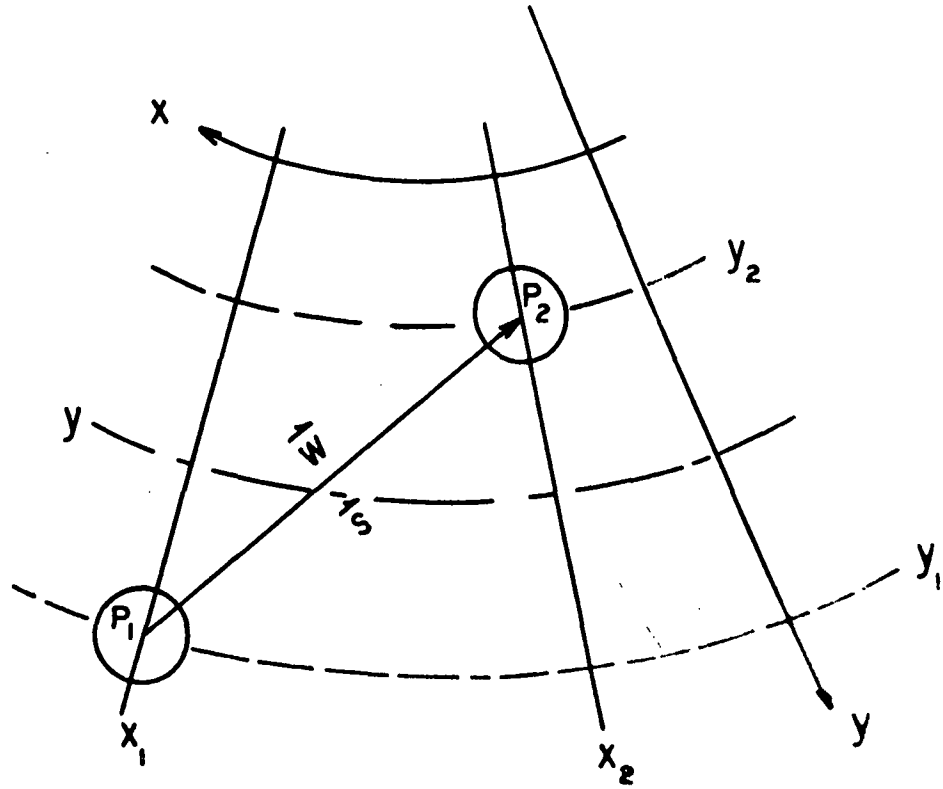


Figure 4. Coordinates of Well Travel

$$\vec{w} = \frac{d\vec{s}}{dt} \approx i \left(\frac{x_2 - x_1}{\Delta t} \right) + j \left(\frac{y_2 - y_1}{\Delta t} \right) \quad (69)$$

In terms of velocity components,

$$\vec{w}(y, t) = iu(y, t) + jv(y, t) \quad (69a)$$

In view of the kind of flow taking place in the Fiber Flexibility Tester (Couette type), the y-component may be identified as the component due to random collision and turbulence, v'. Therefore,

$$v(y, t) = v' = \frac{y_2 - y_1}{\Delta t} \quad (70)$$

where

$$y \approx \frac{y_1 + y_2}{2} \quad (71)$$

The component of travel in the x-direction is due to the velocity component, u, at a time interval Δt . Therefore,

$$u(y, t) = \frac{x_2 - x_1}{\Delta t} \quad (72)$$

with y by Equation (71). The displacements of a large number of balls were measured in this way. To obtain the distribution of the time mean velocity, $\bar{u}(y)$, the coefficients of least-square-error fit polynomials of various degrees were computed by the method of multiple linear regression. It was found that the following third-degree polynomial equation described the data well:

$$\bar{u} = -16.3197 + 19.8286y - 6.4639y^2 + 1.2433y^3 ; \quad (0 \leq y \leq h) \quad (73)$$

where the annulus width $h = 2.54$ cm. The numerical values of the coefficients are such that, e.g., the (fictitious) ball velocity at the inner wall (where $y = 0$)

would be $\bar{u}(0) = -16.3\dots$ cm./sec. The distribution according to Equation (73) is shown in Fig. 5. It is of interest to note that the zero velocity point is located slightly towards the outer cylinder (rather than at the midpoint), indicating a small centrifugal effect. The curve as a whole is S-shaped, which, in view of H. Reichhardt's data for plane Couette flow, is typical in turbulent flow (19). (The reader may recall that the velocity distribution in laminar rotational Couette flow is one without an inflection point.)

In order to obtain the fluctuation, $\underline{u}'(\underline{y}, \underline{t})$, in the rotational direction, we borrowed from Prandtl's mixing-length theory the suggestion of putting

$$\left. \begin{aligned} \underline{u}'(y, t) &= -l \frac{d\bar{u}}{dy} \approx -k'[\bar{u}(y_2) - \bar{u}(y_1)] \\ k' &= k'(y/h, t) \end{aligned} \right\} \quad (74)$$

where \underline{y}_1 and \underline{y}_2 are known from the photographs, so that Equation (73) can be employed. By combining Equations (70) and (74), the product

$$\rho \underline{u}' \underline{v}' \approx \rho k'(y/h, t) [\bar{u}(y_2) - \bar{u}(y_1)] \frac{y_2 - y_1}{\Delta t} \quad (75)$$

is obtained which is representative of the rate of transfer of \underline{x} -momentum in \underline{y} -direction when the balls jump (as a result of turbulent fluctuations) or are being kicked (by the energy of collision impact) from one orbit into another. ρ is the density of the balls, and \underline{k}' is a time- and orbit-dependent unknown function expected to vanish at the cylinder walls. Figure 6 shows the field of $\underline{\rho u' v' / k'}$ points vs. position as obtained by applying Equation (75) to the data.

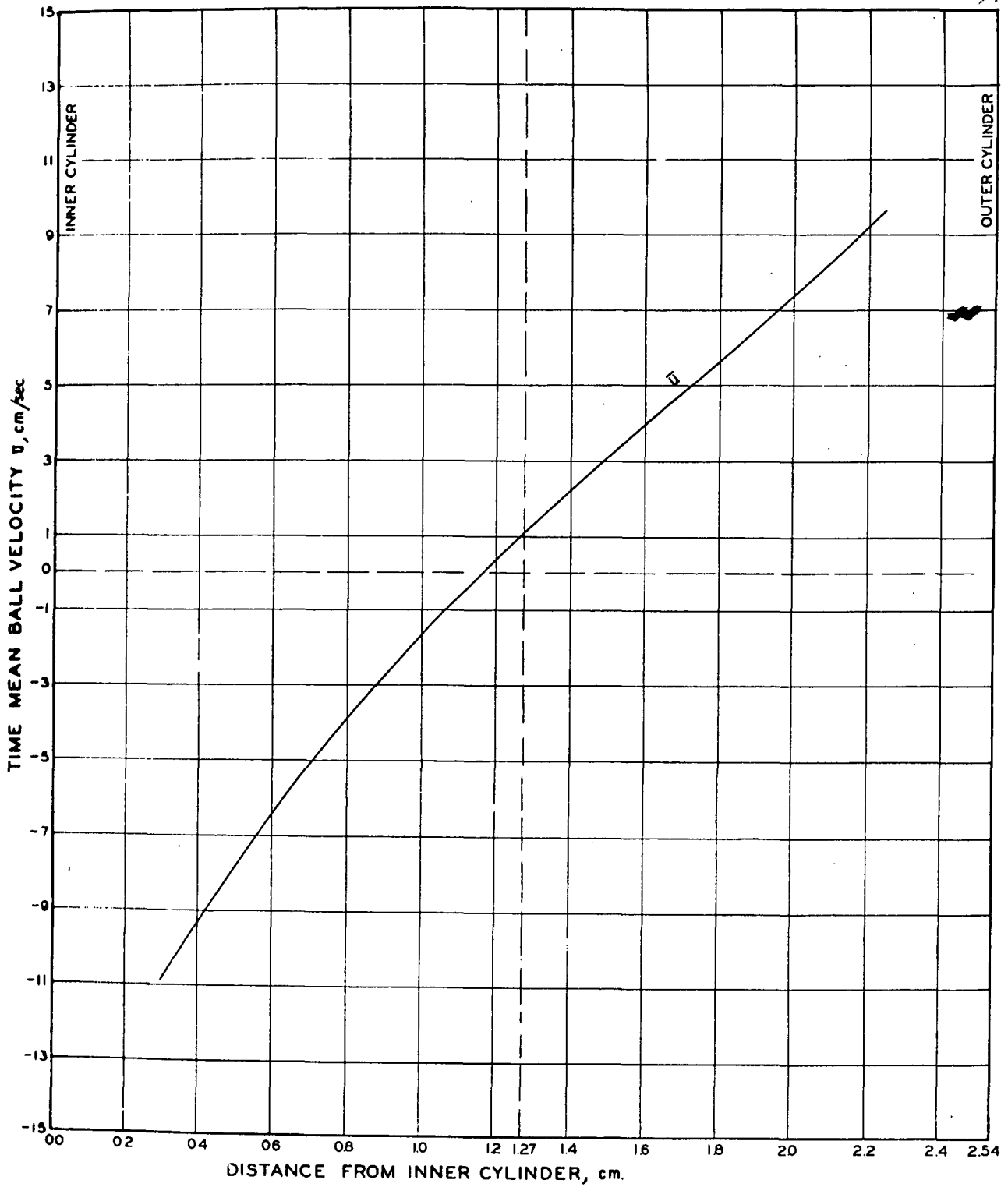


Figure 5. Distribution of Time-Mean Ball Velocity for Fiber Ball-Sirup Mixture in a Rotary Couette Apparatus

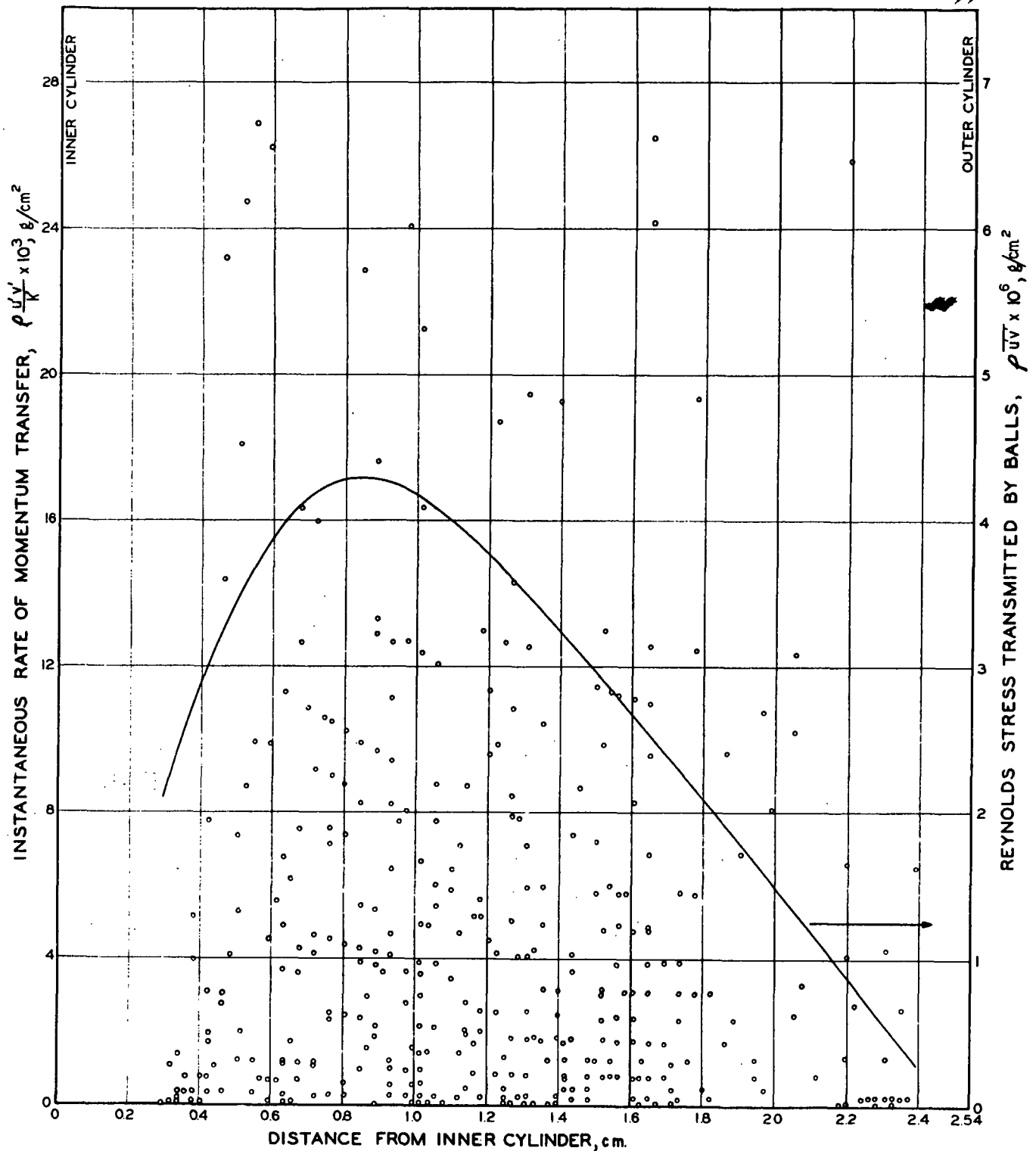


Figure 6. Distribution of Rate of Instantaneous Momentum Transfer by Fiber Balls of Ball-Sirup Mixture in a Rotary Couette Apparatus. Curve Represents Distribution of Time-Mean Value

Although each point would have to be time labeled separately, the result is systematic in a number of aspects: Only less than 1% of all points (not shown) turned out with the opposite sign. At a distance from the cylinder walls of about an average ball's radius, transfer of momentum by the balls ceases because of geometric hindrance. Assuming now that relative flow through the balls was negligible (the well-bonded balls could be considered almost rigid) and further assuming (for the purpose of present convenience because the velocities of the sirup are unknown) that the momentum loss through viscous flow about the balls is of a smaller order of magnitude, turbulent Couette flow would have to follow

$$(\rho_f \overline{u'v'})_{\text{balls}} + (\rho_s \overline{u'v'})_{\text{sirup}} \approx \text{const.} \quad (76)$$

with viscous friction at the walls neglected. The field of ball points appears to indicate that momentum transfer in the wall regions is dominated by that of the fluid, while away from the walls and toward the middle of the field the role of the balls is becoming more significant. The curve contained in Fig. 6 represents an attempt at the distribution of the time mean, $\overline{\rho u'v'}$. Whether such a conclusion is also realized and, for that reason helpful in the analysis of channel and tube flow of fiber suspensions, remains to be shown by future work.

DISCUSSION

Past attempts to approach an understanding of the flow phenomena associated with fiber-water suspensions have been, with few exceptions, based on a premise. It was assumed that by treating the data as if they belonged to a homogeneous Newtonian fluid (for which the means of clever analysis have long been devised), useful and lasting conclusions could be drawn. At best, such attempts helped to categorize or rephrase the description of the observed phenomena, but they were unable to describe and explain the mechanism of fiber-water interaction producing these phenomena.

The present treatment of a suspension of fibers in water as what it actually is--namely, a mixture of two things--leads to a new set of equations. By making the assumption that the fiber phase can be treated as a (quasi) continuum and by omitting the assumption that the fibers (or their agglomerates) move with the same velocity as the water, two continuity and two flow equations are obtained. Their specialization to two-dimensional, steady, fully-developed flow in a Cartesian frame describes the slow flow of a suspension in a flat channel and, in their time-smoothed form, turbulent flow under the same conditions.

At the time of this writing, there was not enough time left to demonstrate more explicitly the results of the analysis. Regarding laminar flow, such a demonstration would have to aim at explaining the position of the friction factor of suspension flow, f , above the water curve in terms of the stress-strain behavior of the fiber network including its dependence on fiber concentration, c , and channel width, h (in case the similarity between tube and channel goes this far). What the analysis shows by way of equations may be summarized as follows:

1. The treatment of steady, laminar, and fully-developed flow as the mutually dependent flow of two phases, i.e., water and fiber, leads to Brinkman-type equations describing the flow of the water phase and to the well-known static equilibrium conditions of the Theory of Elasticity.
2. Under the stress-strain conditions of slow flow, the general form of the established stress-density relationship of fiber mats (Campbell equation) is shown to reduce to Hooke's law stating the fact that strains are directly proportional to stresses.
3. With Hooke's law applying, strains and stresses are reversible and therefore related to one another as known from elasticity theory.
4. In fully-developed channel flow, the network plug experiences negative strains both in flow and in cross direction as well, thus giving rise to a fiber concentration higher during flow than at rest. Consequently, the plug moves with a (constant) velocity slightly lower than that of the water, whose velocity varies from a maximum in the middle to a slightly lower value at the plug boundary, and (within a fiber-free water layer) to zero at the solid channel wall.
5. The strain in cross direction--and thus the thickness of a fiber-free water layer along the solid walls--is flow-rate and consistency dependent; it also depends on the channel width. In its basic dependence on relative flow, the flow mechanism is clearly associated with specific volume and surface of the fibers.
6. All normal stresses are constant within the plug; the shear stress, however, appears to reach its optimal value at the plug surface, and also increases with flow rate.

Regarding the analysis of turbulent flow, its formal state should not distract from the following preliminary findings:

1. The time-smoothed equations of motion are, in general, different from those underlying the conventional treatment of turbulent flow of Newtonian fluids because of the appearance of additional Reynolds stresses (in connection with turbulent mass transfer) and of drag terms whose main effect stems from claimed velocity differences between water and fiber agglomerates. Also, by accounting for the motion of water and fiber separately, the differential order of the system of equations is doubled, thus doubling the number of boundary conditions which can be satisfied.
2. As suggested by closer inspection, these equations apparently reduce into the known equations for Newtonian fluids in the case where a uniform distribution of fibers and equality of fiber and water velocities are approached. These are quite compatible conditions, and there is a possibility for this to occur at higher velocities. The property of fiber suspensions to behave like water upon reaching a certain consistency-dependent Reynolds number has been reported by Seely (13).
3. In order to render the derived equations suitable for numerical solution, the Reynolds stresses must be expressed in terms of the time-mean velocity distribution. Prandtl's mixing-length concept is the model to be profitably used here. Available and new tube-flow velocity data will be helpful in making the right decisions regarding the distribution of the various mixing lengths involved.

4. The important role of the drag term in the analysis of laminar flow has become quite obvious. Its effect in turbulent flow is not less strongly indicated, but the definition of the time-mean resistance is still a matter of continued concern. Consultation of the data may offer means of securing its final form.

ACKNOWLEDGMENT

The considerable work Mrs. E. Cary had in properly spacing and reliably typing the numerous equations and also her frequent advice in the choice of wording are much appreciated.

NOMENCLATURE

$\underline{A}, \underline{B},$ $\underline{C}_1, \underline{C}_2$	=	integration constants
\underline{a}	=	viscous flow resistance of a coherent porous medium, $1/\text{cm}^2$
$\bar{\underline{a}}$	=	time-mean viscous flow resistance of a network fragment or floc, $1/\text{cm}^2$
$\underline{c}, \underline{\rho}$	=	fiber mat density, g_f/cc .
\underline{D}_i	=	drag force per unit volume of mixture, g_f/cc . of mixture
\underline{E}	=	modulus of elasticity, g_f/cm^2 of mixture of a 3-dimensional fiber network
\underline{e}	=	mat volume dilatation, dimensionless
\underline{F}_i	=	component of body force per unit volume of mixture, g_f/cc . of mixture
\underline{f}	=	friction factor of tube flow, dimensionless
\underline{G}	=	shear modulus, g_f/cm^2
\underline{g}_i	=	component of gravitational acceleration in the direction of the \underline{x}_i -coordinate
\underline{h}	=	width of channel, cm.
$\underline{i}, \underline{j}, \underline{k}$	=	unit vectors of a Cartesian system
\underline{k}'	=	nondimensional mixing length
\underline{l}	=	mixing length, cm.
\underline{l}'_e	=	mixing length of turbulent transport of fibers, cm.
\underline{l}'_λ	=	mixing length of turbulent transport of fluid, cm.
\underline{M}_b	=	compressibility constant, $[g_f^{(1-N)} \text{cm}^{(2N-3)}]^{1/N}$
\underline{m}	=	dry mass of fiber mat, g_m
\underline{N}	=	compressibility constant, dimensionless
$\underline{P}(\underline{x}_1, \underline{y}_1),$ $\underline{P}(\underline{x}_2, \underline{y}_2)$	=	point coordinates of fiber ball positions
\underline{p}	=	static pressure of mixture, g_f/cm^2 of mixture
\underline{p}'	=	fluctuation of mixture pressure, g_f/cm^2
\underline{Q}	=	suspension flow rate, cc./sec.

- Re = Reynolds number, dimensionless
 $r(x)$ = radius of floc in position x , cm.
 $\frac{S}{V}$ = specific surface area, $cm.^2/cc.$ of fiber
 s = wall distance, cm.
 t = time, sec.
 u, v = components of velocity vector, \vec{w}
 V = mat volume, cc.
 V_{λ}, V_p = superficial water and fiber velocities, resp., $cm./sec.$
 ΔV = mat volume change, cc.
 $v_{\underline{i}}$ = velocity component in the direction of the $x_{\underline{i}}$ -coordinate, $cm./sec.$
 $v'_{\underline{i}}$ = time-dependent velocity fluctuation, $cm./sec.$
 \vec{w} = velocity vector
 x, y, z = Cartesian coordinates
 $x_{\underline{i}}$ = \underline{i} th coordinates of a Cartesian system
 x_1 = thickness coordinate of fiber plug, cm.
 ϵ = porosity or void fraction, dimensionless
 ϵ_f = mean void fraction of flocculation, dimensionless
 ϵ_r = mean void fraction in a floc of radius r , dimensionless
 K = von Kármán constant
 $\kappa_1, \kappa_2, \kappa_3$ = mixing-length distribution parameters, dimensionless
 μ = viscosity
 ξ, η, ζ = displacements in the directions, resp., of an $x-y-z$ coordinate system, cm.
 ρ = density of the mixture, $g_m/cc.$ of mixture
 σ = Poisson ratio, dimensionless
 $\tau_{\underline{ij}}$ = stress tensor, $g_f/cm.^2$

Subscripts:

- $\underline{i}, \underline{j}, \underline{k}$ = index for components of a Cartesian system
- Λ = index for water, denoting a true characteristic
- λ = index for water, denoting an apparent characteristic in the mixture
- Φ = index for fibers, denoting a true characteristic
- φ = index for fibers, denoting an apparent characteristic in the mixture
- o = index for initial states

LITERATURE CITED

1. Brecht, W., and Heller, H., Tappi 33:14A(1950).
2. Durst, R. E., and Jenness, L. C., Tappi 37:417(1954); 38:193(1955); 39:277 (1956).
3. Daily, J., and Bugliarello, G. M.I.T. Hydrodynamics Laboratory Report No. 30. Cambridge, Mass., Massachusetts Institute of Technology, 1958.
4. Daily, J., and Bugliarello, G., Tappi 44:497(1961).
5. Daily, J., and Chu, T. M.I.T. Hydrodynamics Laboratory Report No. 48. Cambridge, Mass., Massachusetts Institute of Technology, 1961.
6. Robertson, A. A., and Mason, S. G., Tappi 40:326 (1956).
7. Forgacs, O. L., Robertson, A. A., and Mason, S. G., Pulp Paper Mag. Can. 59:117 (1958).
8. Raij, U., and Wahren, D., Svensk Papperstid. 67:5(1964).
9. Robertson, A. A., and Mason, S. G. In Bolam's Formation and structure of paper. Transactions of Symposium at Oxford, Sept., 1961. Vol. 2. p. 791. London, British Paper and Board Makers' Association, 1962.
10. Baines, W. D., Svensk Papperstid. 62:823(1959).
11. Meyer, H., Tappi 47:78(1964).
12. Mih, W., and Parker, J., Tappi 50:237(1967).
13. Seely, Truman. The structure and behavior of flocculated fiber suspensions under hydrodynamic stress. Doctoral Dissertation. Appleton, Wis., The Institute of Paper Chemistry, 1968.
14. Carrasquilla, A. Flow of suspensions of nonspherical particles. Master of Science Dissertation. Cambridge, Mass., Massachusetts Institute of Technology, 1965.
15. Hubley, C., Robertson, A. A., and Mason, S. G., Can. J. Res. B 28:770(1950).
16. Wollwage, J. An investigation of the flocculation of papermaking fibers. Doctoral Dissertation. Appleton, Wis., The Institute of Paper Chemistry, 1938.
17. Emmons, H. W., Tappi 48, no. 12:679-87(1965).
18. Nelson, R. W., Tappi 47, no. 12:752-64(1964).
19. Schlichting, H. Boundary layer theory. New York, McGraw-Hill, 1960.

20. Bird, R. B., Stewart, W. E., and Lightfoot, E. N. Transport phenomena. New York, Wiley, 1965.
21. Sokolnikoff, I. S. Mathematical theory of elasticity. New York, McGraw-Hill, 1956.
22. Han, S. T. The status of the sheet-forming process. Appleton, Wis., The Institute of Paper Chemistry, 1965.
23. Chang, N. L. Unpublished work, The Institute of Paper Chemistry, 1968.
24. Happel, J. A., A.I.Ch.E. Journal 5, no. 2:174(1959).
25. Seely, T., J. Polymer Sci. 5A:3029(1967).
26. Project 2570, Report One. Model studies on fiber flocculation. Appleton, Wis., The Institute of Paper Chemistry, April 20, 1967.

THE INSTITUTE OF PAPER CHEMISTRY

H. Meyer / NLC

H. Meyer, Research Associate
Mechanical Processes Group
Technology Section

N. L. Chang

N. L. Chang, Research Fellow
Mechanical Processes Group
Technology Section